90-2635

Paper No. _____
AN ASAE MEETING
PRESENTATION

RAPID MOISTURE MEASUREMENTS IN THIN SAND SLABS

by

J. Bell, Research Assistant
J.S. Selker, Research Assistant
T.S. Steenhuis, Associate Professor
Department of
Agricultural and Biological Engineering
Cornell University, Ithaca, NY 14853

R.J. Glass, Senior Member of Technical Staff
Sandia National Laboratories
Albuquerque, NM 87185

Written for presentation at the
1990 International Winter Meeting
sponsored by
THE AMERICAN SOCIETY OF AGRICULTURAL ENGINEERS

Hyatt Regency Chicago
Chicago, Illinois
December 18-21, 1990

SUMMARY:
The theoretical basis for the relationship between moisture content and light transmission (FFM) is developed, and shown to correspond well to the observed behavior. A calibration procedure for FFM based on the relationship between moisture content and matric potential is presented and tested. Means of expanding the range of sensitivity of the FFM are discussed.

KEYWORDS:
Calibration, Soil Moisture, Digital Images, Video, Two-dimensional

American Society of Agricultural Engineers

St. Joseph, MI 49085-9659 USA

Introduction

Understanding the processes involved in transport of dissolved chemicals through unsaturated soils is central to the accurate prediction of contaminant loading to groundwater supplies. Although the governing equation for unsaturated flow has been well-known for more than 50 years (Richards, 1931), the effects of non-linearity in the system, as well as heterogeneity make the analytical description of unsaturated flow systems impossible in all but the most ideal conditions. This has lead to the extensive use of physical analogues (e.g., Hele-Shaw cells for saturated flow), and numerical solutions to Richards equation. The development of video image analysis systems has opened a new avenue for the direct observation of flow through unsaturated porous media, where the moisture content at all points in a two-dimensional system can be monitored continuously. We refer to this technique as the full field moisture content measurement technique, or FFM.

Standard methods of soil water measurement are impractical for monitoring the moisture content in continuous two-dimensional flow experiments (Gardner, Walter H., 1986). Gravimetry with conventional or microwave drying requires that the soil samples be disturbed to take measurements. Water content can be measured only one point at a time with gamma ray or neutron attenuation. Measurements by electrical conductivity and capacitance are limited to points determined before beginning the experiment. Neutron thermalization and the Time Domain Reflectomotry (TDR) method measure the average water content of a soil volume and thus cannot distinguish between water contents of two points near to one another. It may be possible to obtain continuous full field measurements by a microwave transmission technique, but such a technique has yet to be developed. The full field light transmission technique is not only a simple technique for continuously measuring water content in a two-dimensional field, but it also allows for visual observation of experiments.

The FFM approach, which was first employed by Glass et al. (1989), is based on the observations of Hoa (1981) that the intensity of light transmitted through a slab of silica sand is strongly dependent on the moisture content of the sample. The increased light transmission arises from the matching of the index of refraction of silica and water. The FFM provides detailed data which allows for extensive investigation of rapidly changing unsaturated flow processes (Glass et al., 1989). Quantitative application of the method has been hampered by the effects of irregular lighting (e.g., near the chamber boundaries), which give rise to local deviations in transmitted light. In addition, the lack of a physical model for the system limited the application of the method to new problems. This paper presents a procedure for correcting for irregular lighting of the sand sample (referred to as normalization) and a simple method to obtain quantitative measurements of moisture content using an FFM system. The range of moisture contents over which the method is sensitive is explored theoretically and experimentally, indicating the potential applications and limitations of the method.

Physical Model

A quantitative understanding of the physical processes which govern the optical properties of semi-wetted transparent porous media provides a foundation from which the FFM technique may be explored and expanded. The dominant features of the dependence of light transmission on moisture content may be captured using a simplified model, which may be compared to the empirically obtained relationship to verify that the mechanism which gives rise to increased transmission with moisture content has been correctly identified.

The development of an exact physical model would require detailed information of the geometry of the media's constituent particles, the inter-particular contact geometries, and other extremely detailed information. Although this information could be incorporated into a numerical simulation of the system, the fundamental properties of the system can be captured analytically through the use of four simplifying approximations. We base our analysis on the following four assumptions:

1) The optical properties of sand particles are reasonably represented by spherical particles of uniform radius (taken as the median media particle radius) arranged in a cubic face centered packing. All light is assumed to strike sand, rather than passing between particles.

2) The light transmitted through the sand slab travels perpendicular to the plane of the slab at all points (i.e., refraction is not considered except as it influences reflection).

3) The fraction of light which is reflected while crossing a boundary between materials is taken as lost.

4) The fraction of light which is reflected while crossing a boundary is independent of the angle of incidence up to the critical angle, at which point all light is taken as reflected. The reflected fraction is obtained from Fresnell's formula for normal incidence.

Approximations 1, 2, and 3 are adopted strictly for reasons of simplicity, and are shown to provide a reasonable result. Approximation 4 is adopted based on theoretical grounds, as is discussed in the following text.

For a typical pair of idealized spherical soil particles of radius, R, joined by a meniscus of water with air/water interface radius of r_2 as shown in Figure 1, the volume of water, V, held in the meniscus is given by Kirkham and Powers (1972)

$$V = \left[\frac{4\ \pi\ R^3}{3}\right][A(B - D + M) + N] \qquad (1)$$

where $A = (3\gamma^4/32)(1-\gamma)^3$, $B = \cos\beta(4-4\gamma+\gamma^2)$, $D = (2\gamma-\gamma^2)(\cos\beta\sin^2\beta + 2\cos\beta)$, $M = (\gamma^2/3)(\cos\beta\sin^2\beta + 2\cos\beta)$, $N = (1/4)(\cos\beta\sin^2\beta + 2\cos\beta - 2)$, and $\gamma = r_1/R$. If cubic packing of the particles is assumed (Figure 2), the volumetric moisture content, θ, of a soil made up of such particles is

$$\theta = \frac{3V}{8\ R^3} \qquad (2)$$

Equations (1) and (2) provide the relationship between meniscus contact angle β, and volumetric moisture content of the soil, θ.

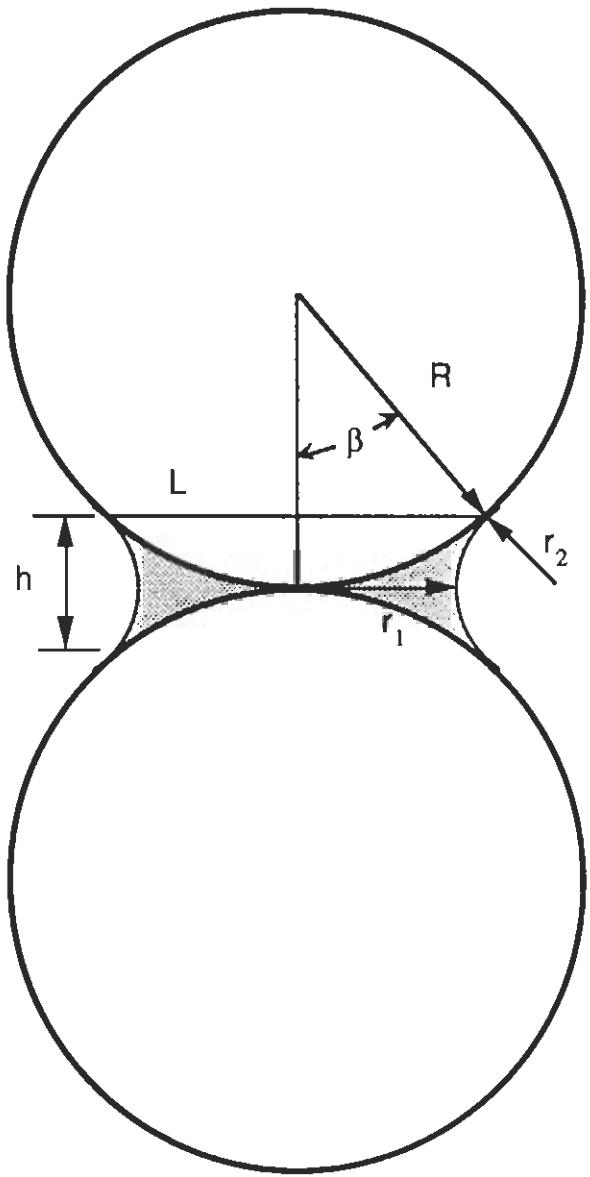

Figure 1: Schematic of idealized spherical soil grains and meniscus connecting the grains (following the notation of Kirkham and Powers, 1972).

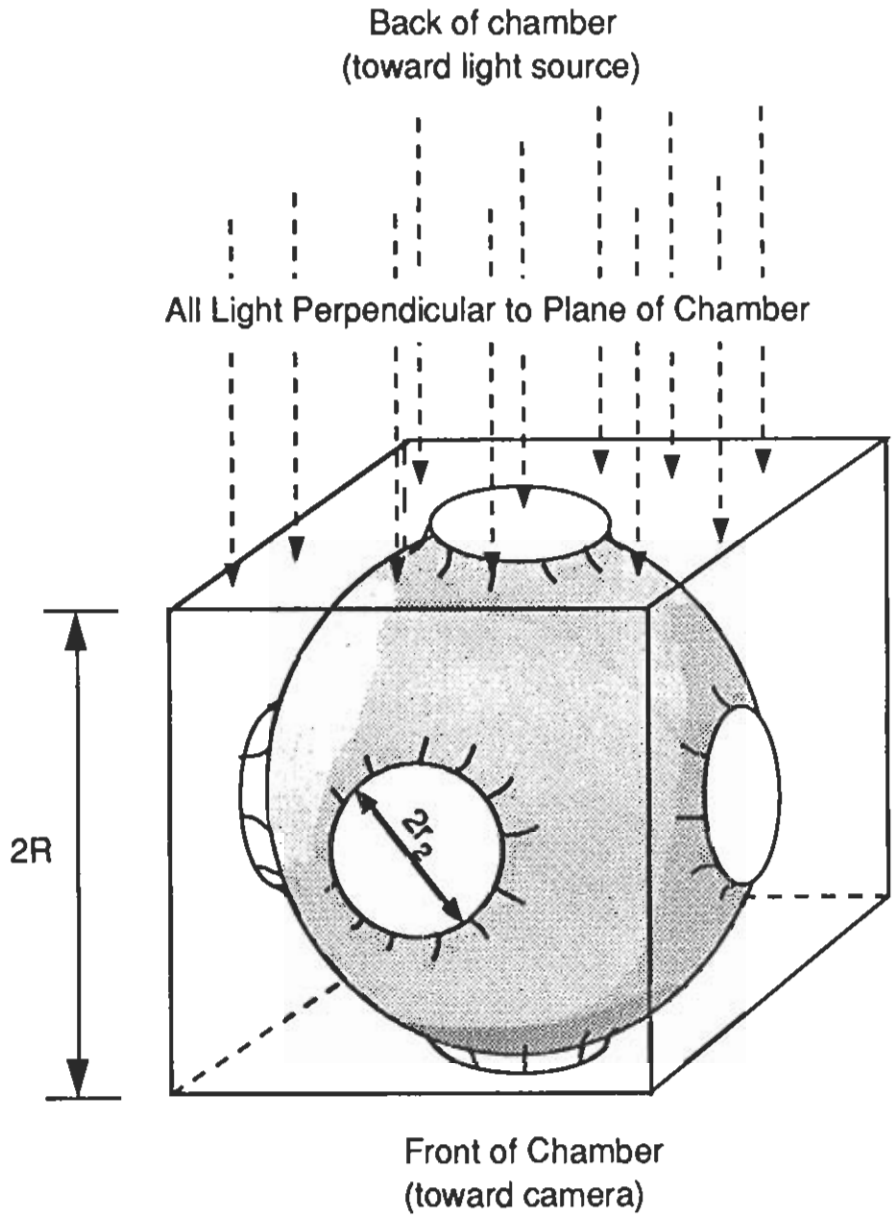

Figure 2: The representative elementary volume for the system. The volumetric moisture content is calculated as the ratio of meniscus and particle volume (Equation (2)).

Figure 3 shows the fraction of light reflected from silica/water and silica/air interfaces as calculated using Fresnel's formula (Handbook of Chemistry and Physics, 1987). This formula is approximate, not accounting for the effects of polarization, which, as discussed by Griffiths (1989), give rise to different fractions of light reflected depending on the relationship between the plane of the interface and the plane of polarization. Fresnel's formula, taken with approximation 4, indicates that the reflected fraction of light from air/silica and silica/air boundaries is 0.04 with silica/water and water/silica reflected fraction being 0.0036. At angles greater than or equal to the critical angle, α_c,

$$\alpha_c = \sin^{-1}\left(\frac{n_2}{n_1}\right) \tag{3}$$

all of the light passing from high index of refraction (n_1) to low index of refraction (n_2) is reflected internally, as indicated in Figure 3, and hence taken as lost (assumption 3) in this calculation.

Following assumption 1, the number of interfaces n which a light ray will transect through a chamber of thickness T is

$$n = T/R \tag{4}$$

From assumptions 2 and 3 and Fesnel's Formula, with no water in the system, 96% of the incident light passes through each air/silica interface, up to the critical angle, 41°, above which all the light is internally reflected. Hence, the minimum light passing through the dry chamber, I(0,x,y), is given by

$$I_{dry}(x,y) = \frac{I_o(x,y) \text{ x Fraction Transmitted x Area of Transmission}}{\text{Area of Particle}}$$

$$= I_o(x,y)\ \frac{(0.96^n)\ \pi\ (R\ \sin(41))^2}{\pi\ R^2}$$

$$= I_o(x,y)\ 0.96^n\ \sin^2(41) \tag{5}$$

where $I_o(x,y)$ is the incident light intensity at the location (x,y) on the back of the sand slab. The incident light intensity would be constant in the case of completely uniform lighting. We take the light intensity to be a function of position for sake of generality. The maximum transmission of light will occur when the water meniscus makes contact with the particle such that rays exit at α_c for the silica/water interface, 62.5° (see Figure 4). Water which makes contact with the soil at an angle greater than 62.5° has no influence on the transmitted light, since light impinging at an angle greater than this is entirely internally reflected. Hence, the light transmitted through the chamber at saturation ($\theta = 1$) is given by

$$I_{sat}(x, y) = I_o(x,y)\ \ 0.9964^n\ \sin^2(62.5) \tag{6}$$

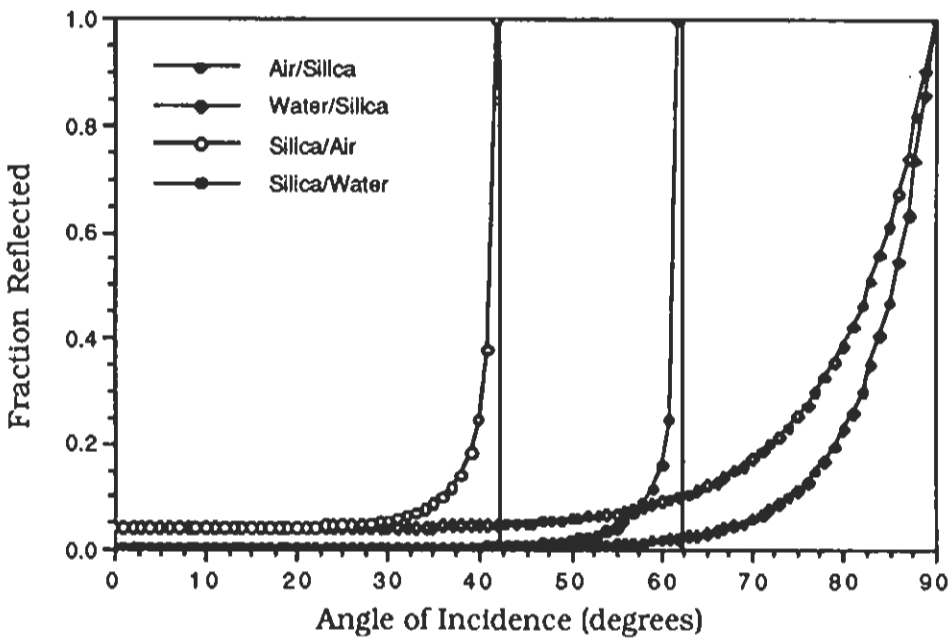

Figure 3: The fraction of reflected light at air/silica, water/silica, silica/air and water/silica interfaces as calculated using Fresnel's formula. The critical angles for silica/air (41.8°) and silica/water (62.5°) are indicated by vertical lines.

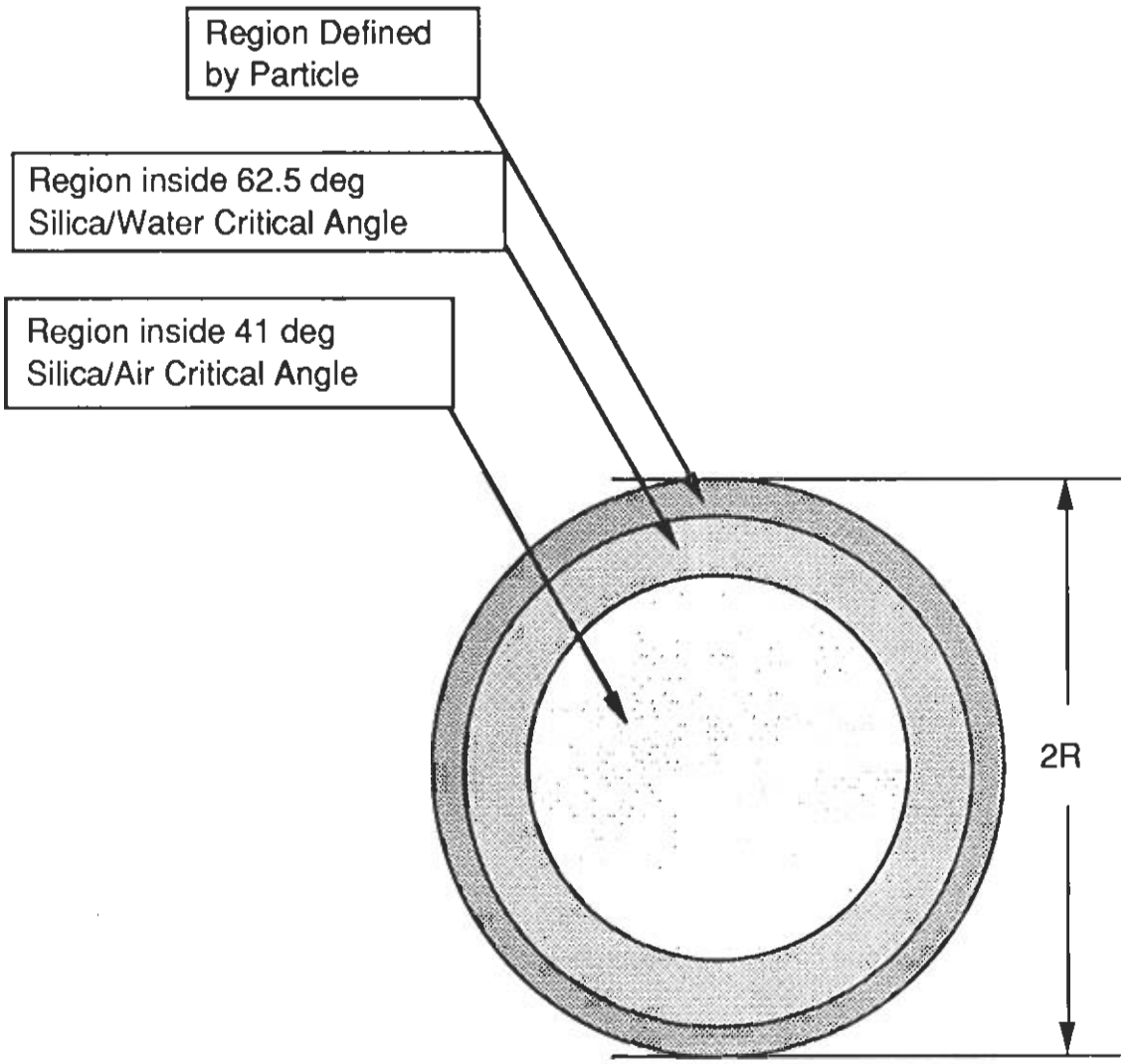

Figure 4: Top view of the system REV, showing the regions of transmission given the critical angles for silica/air and silica/water interfaces.

To estimate the light transmitted at intermediate degrees of saturation, we calculated transmitted light as the sum of light transmitted through water contact interfaces and air contact interfaces. The light transmitted through interfaces connected by water, $I_{wat}(\theta,x,y)$, is

$$I_{wat}(\theta,x,y) = I_o,(x,y)\ 0.9964^n \sin^2(\beta) \qquad \beta \leq 62.5^\circ \qquad (7)$$

While intensity of light transmitted through the interface connected by air is

$$I_{air}(\theta,x,y) = I_o(x,y)\ 0.96^n \left[\sin^2(41) - \sin^2(\beta)\right] \qquad \beta \leq 41^\circ$$

$$I_{air}(\theta) = 0 \qquad \beta \geq 41^\circ \qquad (8)$$

with the total transmitted light given by the sum of the two components

$$I(\theta,x,y) = I_{air}(\theta,x,y) + I_{wat}(\theta,x,y) \qquad (9)$$

Equations (6), (7), (8) and (9) provide a prediction for the relationship between volumetric moisture content and the light intensity measured at the surface of the experiment.

$$I(\theta,x,y) = I_o(x,y) \left\{ 0.96^n \left[\sin^2(41)-\sin^2(\beta)\right] + 0.9964^n \sin^2(\beta) \right\} \qquad \beta \leq 41^\circ$$

$$I(\theta, x, y) = I_o(x,y)\, 0.9964^n \sin^2(\beta) \qquad 41^\circ < \beta < 62.5^\circ$$

$$I(\theta, x, y) = I_o(x,y)\ 0.9964^n \sin^2(\beta) \qquad \beta \geq 62.5^\circ$$

(10)

Where β is a one-to-one function of θ given in Equations (1) and (2).

Correcting for Irregular Lighting

In the preceeding discussion we have maintained notation which explicitly identifies the incident light intensity as a function of position in the chamber (x,y). This follows our own observations that, despite concerted efforts to achieve uniformity in lighting, shadowing at the chamber edges is impossible to completely overcome. To allow full field measurement of moisture content requires a procedure which corrects for non-uniform illumination.

Consider a typical point (x,y) on the surface facing the data collection system for which the intensity of transmitted light through the dry sample is I(0,x,y) and the saturated transmission intensity is $I_{sat}(x,y)$. For any moisture content $0 \leq \theta \leq 1$, the observed light intensity at position (x,y) is given by Equation (10) as $I(\theta,x,y)$. The normalized light intensity at (x,y) was defined by Selker et al. (1989) as

$$I_n(\theta) = \left[\frac{I(\theta,x,y) - I_{dry}(x,y)}{I_{sat}(x,y) - I_{dry}(x,y)}\right] \qquad (11)$$

For any position in the chamber $I_n(\theta)$ is a function of moisture content only, ranging from 0 to 1 between dry to saturated conditions. In practice, the calculation indicated in Equation (11) is straightforward, employing images of the chamber when dry and saturated. The calculation is carried out for each pixel of the video record for each time step to obtain the complete, normalized, experimental record. Some care must be used in applying this result to specific experimental conditions since in this derivation it is assumed that the light transmitted at any position (x,y) depends only on the absorption for the particles on the line through the chamber at position (x,y). In reality, the light follows a diffuse path through the chamber, hence, the intensity at a point on the chamber face reflects the moisture content in some small region about that point. This may lead to deviations from Equation (11) in regions of steep moisture gradient.

Scaling

Miller and Miller (1956) scaling theory can be used with excellent results to relate the characteristic draining curves of similar sands, as is discussed below. If sands are similar in the sense of Miller and Miller, the geometry of the water/sand/air interfaces will be geometrically equivalent at a given moisture content (Figure 2 of Miller and Miller, 1956). The difference in light transmission between the similar sands predicted by Equation (10) may be used to translate the calibration curve for one sand into the expected calibration curve for alternate sands using the relationship

$$F_2(\theta) = F_1(\theta)\frac{I_2(\theta)}{I_1(\theta)} \qquad (12)$$

where subscripts 1 and 2 denote the calibrated and to be calibrated sands respectively, with $I_1(\theta)$ and $I_2(\theta)$ the predicted normalized transmission values from Equation (11), $F_1(\theta)$ being the empirically measured intensity/moisture content calibration curve, and $F_2(\theta)$ being the predicted calibration relation. To apply this procedure requires that approximately the same section of the dynamic range of the video camera is used, to avoid effects not captured by Equation (11).

Application of FFM to Solute Movement in Saturated Soils

This paper is primarily concerned with the application of the FFM technique to the study of unsaturated soils, however another significant application of the method is in the study of transport through saturated soils (aquifers). In this application the transmitted light intensity may be attenuated using a dye solution. Correction for uneven illumination would be achieved using a normalization procedure as presented for moisture content, but using no-dye, and full concentration images in place of dry and saturation images used above. The use of FFM in saturated conditions could prove very valuable in determining solute fate under saturated conditions.

Empirical Calibration

The relationship between the sample's moisture content and the fraction of light transmitted, defined as $I_n(\theta)$ in Equation (11), may be obtained empirically by comparing the light transmitted through a drained slab of sand with the soil's characteristic draining curve as illustrated in Figure 5. In this procedure, the light intensity at a particular elevation (pressure) observed in a FFM slab of sand drained from saturation is associated with the moisture content at that pressure found in a column draining experiment (Figure 5). In this way the intensity is found as a function of moisture content for the particular sand and FFM chamber being calibrated.

Materials and Methods

The FFM chamber and light configuration employed in this study are the same as described by Glass et al. (1989). In the present case, the light transmitted through a sand sample is recorded using standard VHS equipment, providing a field of 512 by 480 data points 30 times per second. Each data point is recorded as a gray level, with a value between 0 and 255. The images collected are then digitally analyzed using video analysis hardware installed in a 80286 IBM AT compatible micro-computer.

The characteristic draining curve is obtained using the segmented column shown in Figure 6. The conditions of packing and infiltration must be identical in the column and FFM chamber to achieve an accurate calibration. The present experiments are conducted with both the FFM chamber and segmented column being filled through a series of randomizing screens. After packing, the samples are purged of air by feeding water soluble CO_2 gas through the ports in the bottom of the chamber and column. The samples are then flushed with de-aired water, leaving no gas filled voids. Video images are made of the FFM chamber when dry, saturated, and after 2 days of drainage, providing the data required in Equation (11) to generate the curve shown in the left-hand frame of Figure 5.

The soil's characteristic draining curve is determined from three repetitions of the column draining experiment, which are shown in Figures 7 and 8 for 40-50 and 20-30 sands (here 20-30 sand is silica sand which passed through a standard 0.850 mm opening No. 20 sieve but was retained by a 0.590 mm No. 30 sieve, with 0.425 mm and 0.295 mm openings for 40-50 sand). All of the sand was prepared by sieving and then washing with a dilute solution of PEX laboratory cleanser followed by 3 rinses with tap water and 2 rinses with distilled water. The sand was agitated by pressurized air injection at each stage in the washing process. The repeatability of the experiment appears quite good from Figures 7 and 8. An analytic expression was fit to each of the curves using least squares to provide a continuous relationship between moisture content and matric potential for the two sands draining from saturation.

Results and Discussion

The sand we employ is well sorted, with a small range of radii, hence the average of the smallest and largest particles in the sample is a reasonable measure of the sand's characteristic radius, R. The predictions for normalized light transmitted through 20-30 and 40-50 silica sands with characteristic radii of 0.72 and 0.36 mm are given in Figure 9.

The calibration curves obtained empirically for the two sands are of similar shape (Figure 10). The most significant feature of the curves is the range over which transmitted light is affected by changing moisture content. In each of these calibrations we see that moisture content above 15% does not significantly increase the transmitted light. The sands tested have saturation volumetric moisture

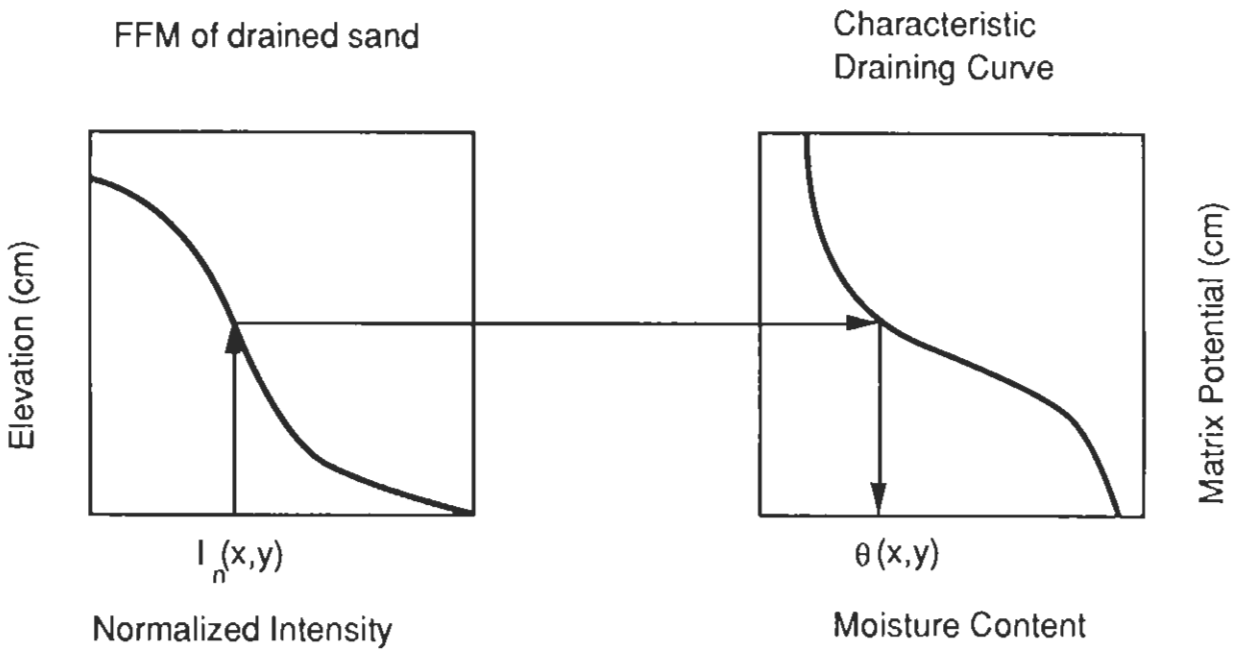

Figure 5: Illustration of FFM calibration based on the soil characteristic draining curve and FFM image of drained chamber.

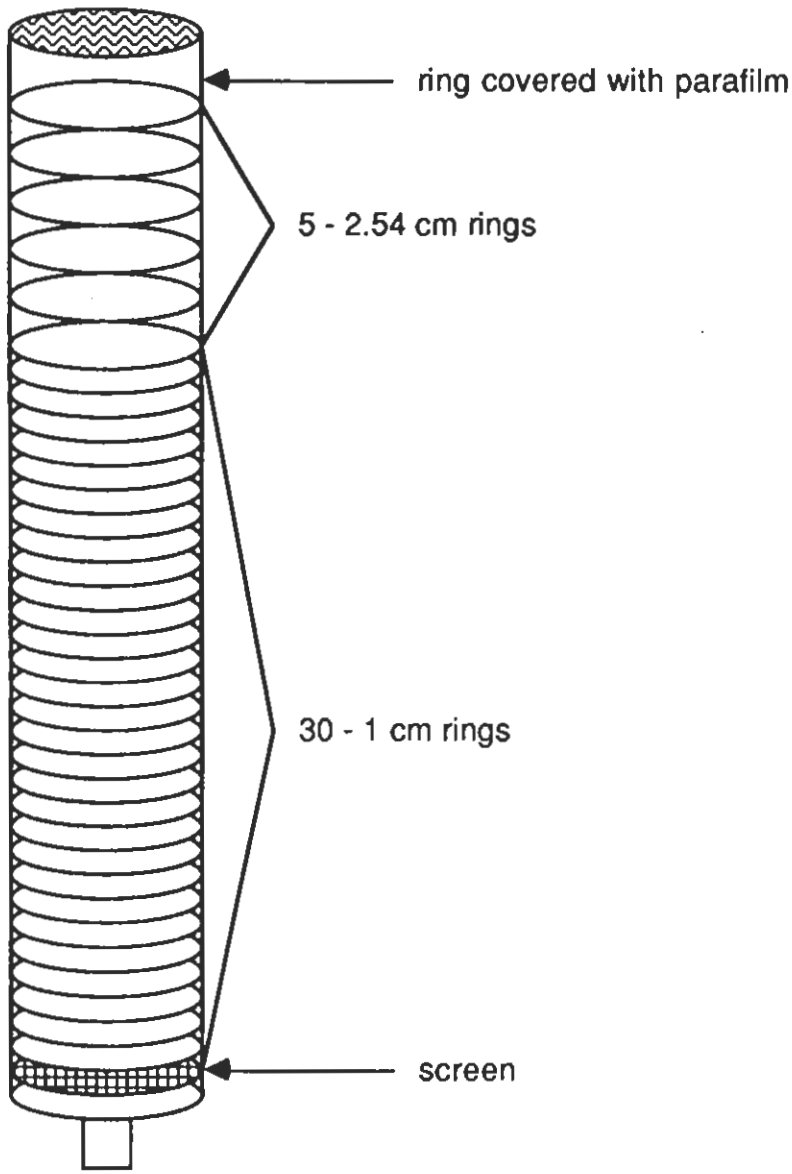

Figure 6: The segmented cylindrical column employed to obtain the θ(h) relationship for sand draining from saturation.

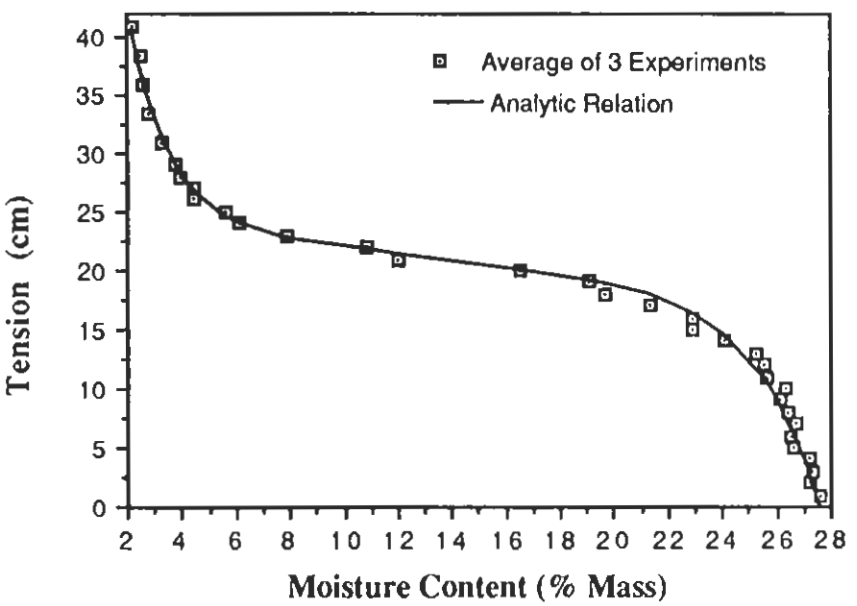

Figure 7: Results of three repetitions of drainage experiments using 40-50 sand. The data points shown are averages of the three values obtained for each tension. The curve shown represents the analytical expression used to relate tension and moisture content.

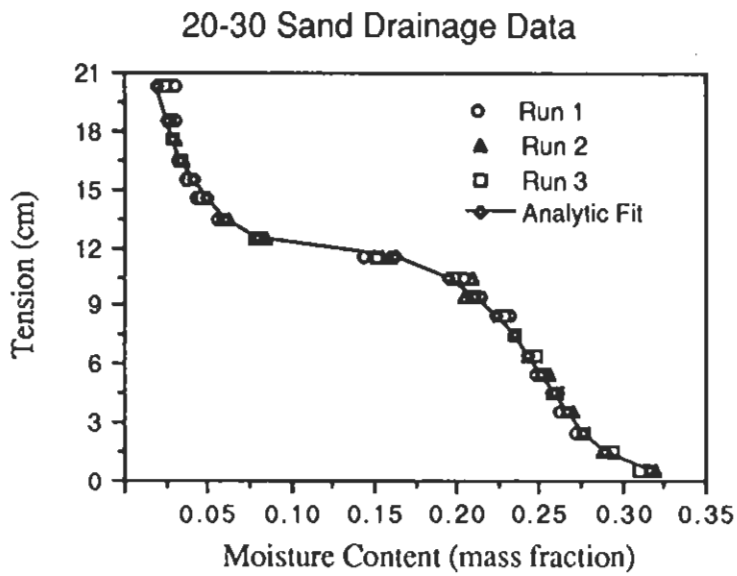

Figure 8: Results of three repetitions of drainage experiments using 20-30 sand. The curve shown represents the analytical expression used to relate tension and moisture content, with points indicating the result of three runs of a column draining experiment.

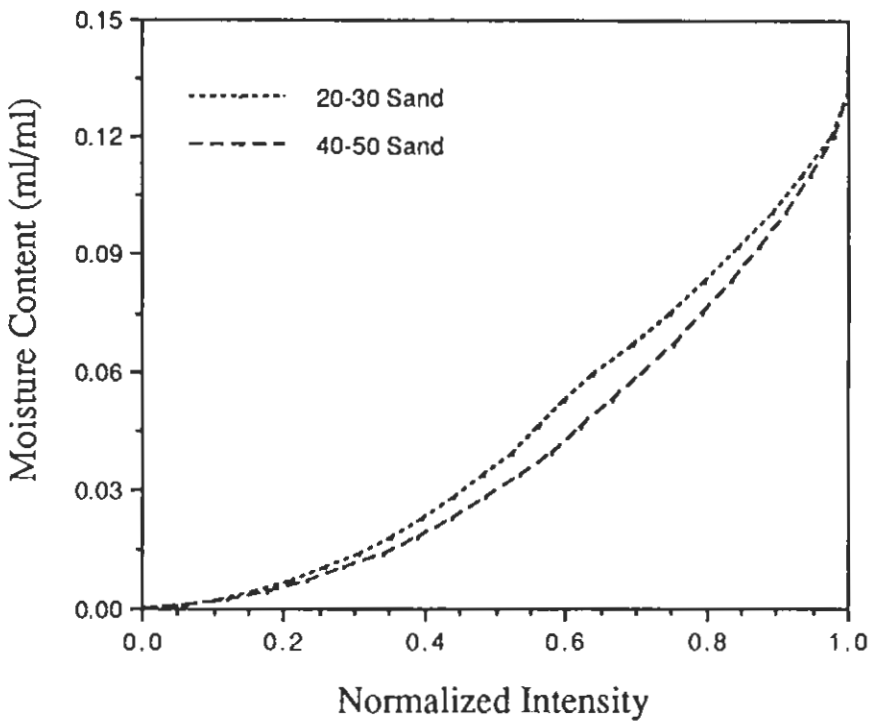

Figure 9: Normalized transmitted light as a function of moisture content calculated using Equation (10).

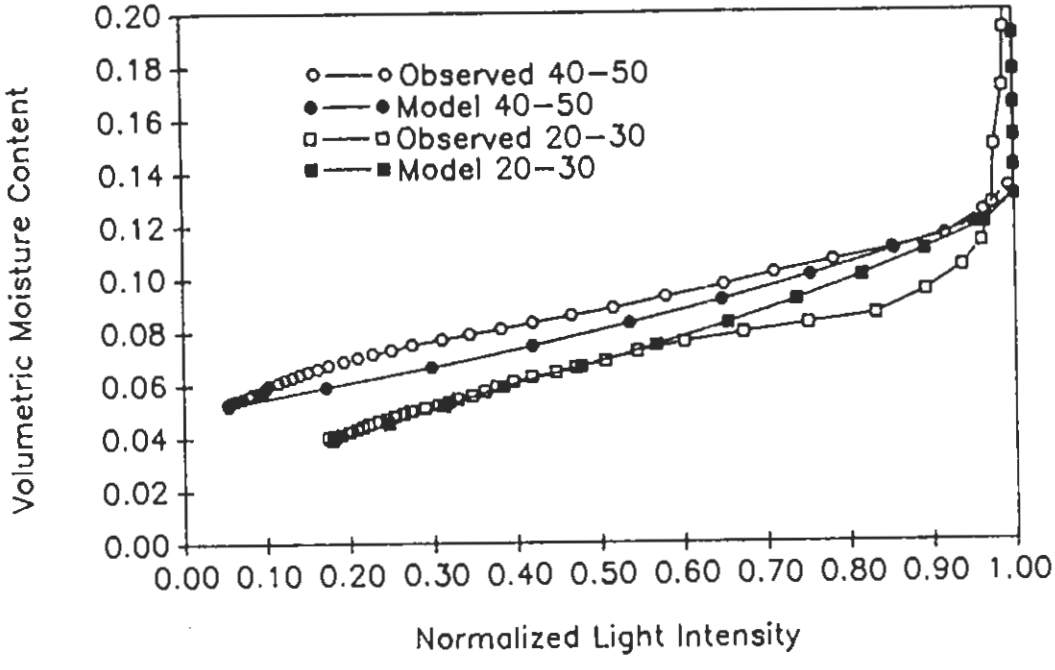

Figure 10: Empirical calibration curves obtained for 20-30 and 40-50 sands are shown with open symbols. The calibration curves shown were obtained from the spherical particle model and have been normalized to the minimum water content observed in the experimental calibrations.

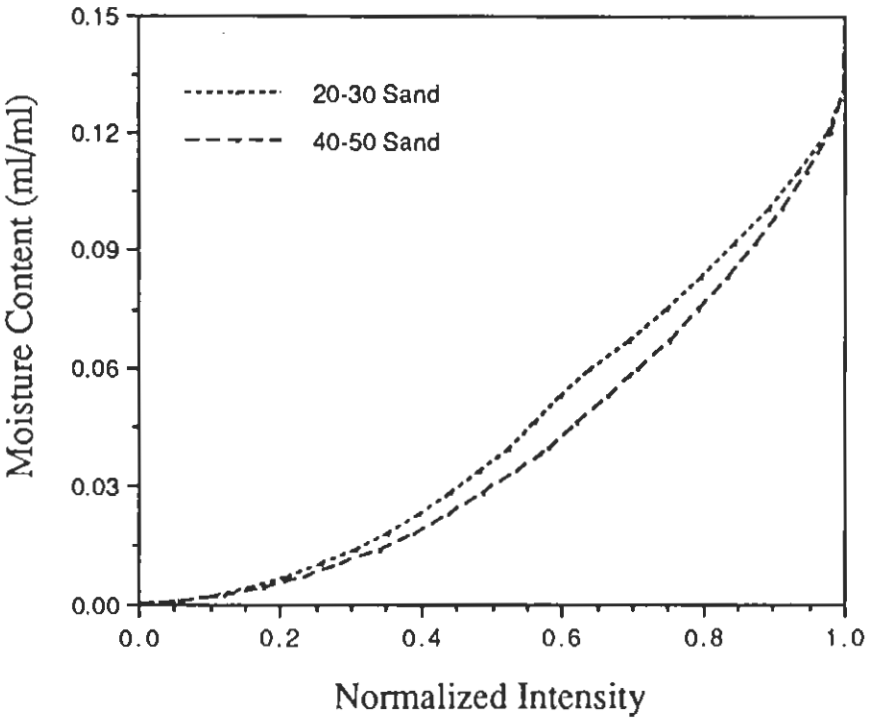

Figure 9: Normalized transmitted light as a function of moisture content calculated using Equation (10).

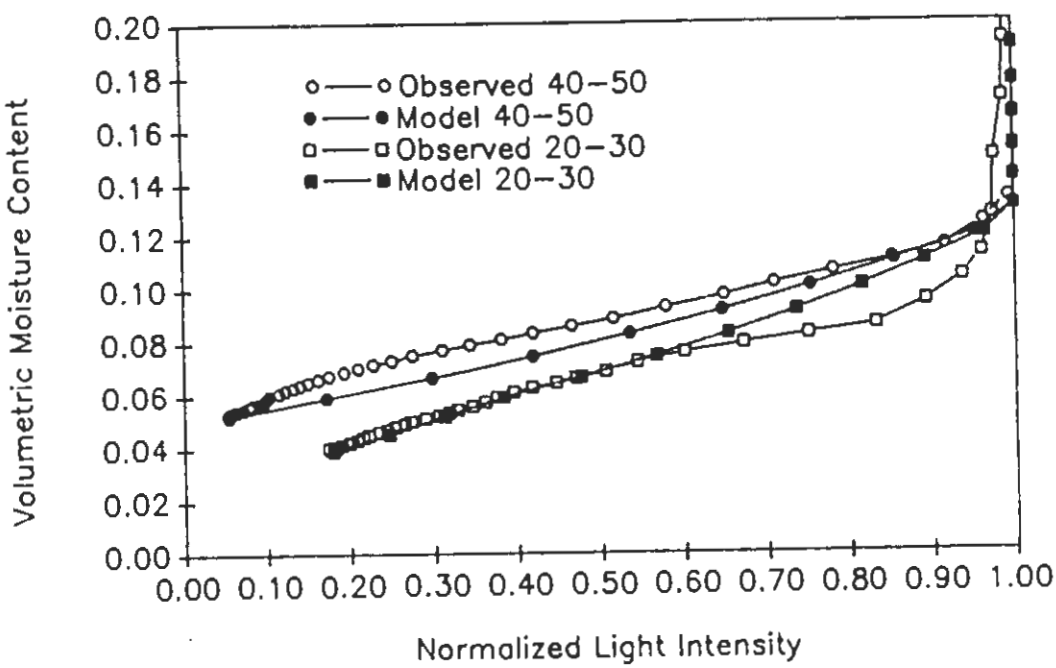

Figure 10: Empirical calibration curves obtained for 20-30 and 40-50 sands are shown with open symbols. The calibration curves shown were obtained from the spherical particle model and have been normalized to the minimum water content observed in the experimental calibrations.

contents of approximately 41% and irreducible moisture contents of approximately 4.4%, indicating that the FFM only gives moisture content data over about one quarter of the range of possible moisture contents in the soil. Figure 10 suggests that the effects of light passing through interfaces between materials of differing indices of refraction have been correctly identified as the mechanism which attenuates light intensity as it passes through the silica sand slab. Equation (10) suggests that if a liquid with the same index of refraction as silica were employed in place of water, the range of moisture content measurement possible using FFM could be expanded. Aqueous solutions of sucrose ($1.33 < n < 1.5$) and calcium chloride ($n = 1.44$) could be investigated in this regard, yielding critical angles approaching 90° (Table 1).

Table 1 Index of refraction for materials related to this study (Handbook of Chemistry and Physics, 1987).

Material	Index of Refraction
Air	1.00
Water	1.33
Aqueous Sucrose	1.33 - 1.50
Aqueous $CaCl_2$	1.44
SiO_2	1.45
Quartz	1.5

The calibration procedure yields quantitative measurements with variable uncertainty, depending on the range of interest. The procedure is susceptible to error from two sources. First, the draining characteristic curve is sensitive to variability in column packing. From Figure 7, which shows three repetitions of the draining experiment for 40-50 sand, the variability is apparent, being most extreme in the 15-41% moisture content region. Referring to the 4-15% region, which may be distinguished using the FFM technique, we see variability of up to 6% between runs, with 20-30 sand variability of less than 1% (Figure 7). An analytic expression was used to translate between pressure and moisture content derived from the draining experiments. The maximum deviation from 3-run average moisture content and the analytical relationship for 40-50 sand is +2.1%, and is -0.8% at p = 21 cm (Figure 7). The maximum deviation for 20-30 sand is 0.6% at p = 13.5 cm (Figure 8). The deviation between three run average moisture content and the fit curve give average discrepancy of 0.09% and 0.2%, and standard deviation between model and experimental results of 0.47% and 0.38%, for 20-30 and 40-50 sands, respectively, for the section of the draining curve required for calibration. Because the scatter in the data is to either side of the fitted curve and the draining results converge to some central curve, it is reasonable to surmise that the relationship between pressure and moisture content determined in these experiments is accurate to $\pm$ 0.5%. Additional systematic error could arise from differences in packing between the column and slab experiments, although the bulk densities of the packings were found to be the same in these experiments.

The similarity in the shapes of the calibration curves suggests the scaling of the results found for these sands to extrapolate calibration curves for other sands, as discussed above. Miller and Miller (1956) scaling theory can be used with excellent results to relate the characteristic draining curves of the two sands employed (Figure 11). To apply this procedure requires that approximately the same section of the dynamic range of the video camera is used, to avoid effects not captured by Equation (10). The vertical shift between the calibration curves is thought to result from the non-linear response of the video camera: the video camera read light levels of 0 for all moisture contents below 5.5% due to insufficient low light sensitivity. By using a more sensitive camera which would allow matching saturated sand light intensity through adjustment of the camera's aperture, we expect that much of this shifting could be avoided, allowing useful application of Equation (12).

Conclusions

FFM was made practical by the advent of widely available video image processing equipment and analysis software. The technique is accessible to many research laboratories, and the equipment used can be applied to analyze results from a wide range of experiments which include visual data. Given the high temporal and spatial resolution and low cost of the FFM technique, we expect this set of tools to be employed by many researchers and educators interested in flow through the vadose zone and saturated soils.

The normalization and calibration procedures presented are readily conducted, and significantly expand the utility of the FFM method. The data obtained using FFM is shown to yield quantitative moisture content data for low moisture content conditions over a broad enough range to be useful in investigating the performance of mathematical models for transport through the vadose zone. The simple physical model proposed explains the observed performance of the system, and allows extrapolation of empirical calibration results using similarity theory. The physical model also suggests the use of high index of refraction aqueous solutions to expand the range of sensitivity of the technique.

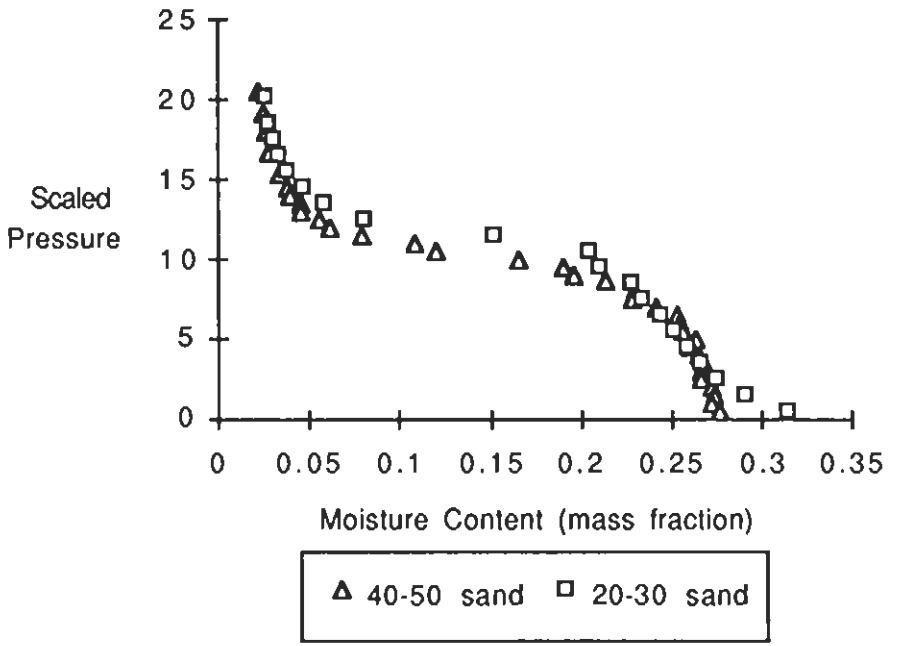

Figure 11: Plot of characteristic scaled draining curves for 20-30 and 40-50 sands using average values from three repetitions shown in Figures 7 and 8.

References

Glass, R. J., T. S. Steenhuis, and J.-Y. Parlange, Mechanism for Finger Persistence in Homogeneous, Unsaturated, Porous Media: Theory and Verification, Soil Sci., 148(1): 60-70, 1989.

Gardner, W. H., "Water content," Methods of Soil Analysis, Part I - Physical and Meralogical Methods, second edition, A. Klute, No. 9 (Part 1) in the series Agronomy, pp. 493-544, American Society of Agronomy, Inc. and Soil Science Society of America, Inc., Madison, WI, 1986.

Griffiths, D. J., Introduction to Electrodynamics, second edition, 532 pp., Prentice Hall, Englewood Cliffs, NJ, 1989.

Hoa, N. T., A New Method Allowing the Measurement of Rapid Variations of the Water Content in Sandy Porous Media, Wat. Resour. Res., 13(6): 992-996, 1981.

Kirkham, D. and W. L. Powers, Advanced Soil Physics, 534 pp., Robert E. Krieger Publishing Co., Malabar, FL, 1984, copyright 1972, J. Wiley and Sons.

Miller, E. E. and R. D. Miller, Physical Theory for Capillary Flow Phenomena, J. Appl. Phys. 27: 324-332, 1956.

Richards, L. A., Capillary Conduction of Liquid Through Porous Mediums, Physics, 1, 318-333, 1931.

Selker, J. S., T. S. Steenhuis and J. -Y. Parlange, Preferential Flow in Homogeneous Sandy Soils without Layering, ASAE paper # 89-2543, 23 pp., American Society of Agricultural Engineers, St. Joseph MI, 1989.

Weast, R. C. Editor, CRC Handbook of Chemistry and Physics, CRC Press, Boca Raton, FL, 1987.